ELSEVIER

Journal of Nuclear Materials 290–293 (2001) 448–453

journal of nuclear materials

www.elsevier.nl/locate/jnucmat

Tritium detection in plasma facing component by imaging plate technique

K. Miyasaka [a], T. Tanabe [b,*], G. Mank [c], K.H. Finken [c], V. Philipps [c], D.S. Walsh [d], K. Nishizawa [e], T. Saze [e]

[a] *Department of Nuclear Engineering, Graduate School of Engineering, Nagoya University, Furo-cho, Chikusa-ku, Nagoya 464-8603, Japan*

[b] *Center for Integrated Research in Science and Engineering, Nagoya University, Furo-cho, Chikusa-ku, Nagoya 464-8603, Japan*

[c] *Institut für Plasmaphysik, Forschungszentrum Jülich GmbH, EURATOM Association, Trilateral Euregio Cluster, 52425 Jülich, Germany*

[d] *Department 1111, Sandia National Laboratories, P.O. Box 5800, Albuquerque, NM 87185, USA*

[e] *Radioisotope Center, Nagoya University Furo-cho, Chikusa-ku, Nagoya 464-8603, Japan*

Abstract

Tritium imaging plate technique (TIPT) has been successfully applied to measure the tritium areal distribution on various graphite tiles used as limiters in TEXTOR. It is observed that tritium distribution on the ALT-II tile is quite homogeneous and different from deuterium distribution and the tritium in redeposited layer is rather small. Such tritium distribution on the graphite tiles in TEXTOR behaves different compared to those in JET and TFTR where tritium was used as fueling gas or NBI injection. In JET and TFTR the tritium is part of the fuel and is co-deposited and retained in a similar manner as the deuterium. In a device like TEXTOR, the high-energy tritons are decoupled from the thermalized deuterons and show different behavior of retention; the main retention mechanism is deep implantation rather than co-deposition with eroded carbon on redeposition-dominated areas. It is also found that the tritium distribution measurements give useful new information on plasma-wall interactions.

Keywords: Tritium mapping; Tritium areal distribution; Imaging plate; Tritium retention; Plasma facing materials; Plasma–surface interaction

1. Introduction

Tritium retention in plasma facing materials is one of the most important safety issues [1]. After the use of tritium in JET and TFTR, the immediate retention was about 40% and 51%, respectively [2,3]. Even after the excessive tritium removal procedure applied to both machines (D-operation, D_2 and He-glow, O_2-venting), remaining long-term tritium retention of ~16% and ~13%, respectively, was observed. A large set of wall tiles have been analyzed afterwards for the deuterium and tritium content. There are various ways for tritium detection such as nuclear reaction analysis (NRA) by means of external ion beam, gas transfer to ionization chamber, chemical transfer into liquid phase and detection by scintillation counter, tritium-β-rays induced X-rays spectrometry (BIXS) and so on. Although most of these methods can detect some parts of the long-term tritium retention, a complete matching of the retained tritium distribution with the extrapolation from the point measurements is not possible, indicating either tritium retention on non-accessible regions in the vessel or a non-uniform toroidal distribution. Therefore, these methods are not suitable for investigation of the tritium areal distribution, and its complete mapping has not been performed yet while it is mandatory.

* Corresponding author. Tel.: +81-52 789 5157; fax: +81-52 789 5157.

E-mail address: tanabe@cirse.nagoya-u.ac.jp (T. Tanabe).

0022-3115/01/$ - see front matter
PII: S0022-3115(00)00513-4

For the investigation of the tritium distribution on material surfaces, tritium autoradiography has been powerful technique and thus applied to study the hydrogen behavior in metals [4]. Recently, an imaging plate technique, which measures the areal distribution of radioactivity with high resolution and ultrahigh sensitivity, based on photo-stimulated luminescence [5,6], has been developed and now enables even ^{40}K mapping in natural foods [7]. In this paper, we have applied the tritium imaging plate technique (TIPT) to determine the tritium areal distribution on in-vessel components used as limiter tiles of TEXTOR-94 and demonstrated that TIPT is not only very useful but also giving a lot of information on plasma-wall interactions.

2. Experimental

Graphite samples investigated in this study were taken from three different types of limiters used in TEXTOR-94, two graphite tiles (tile nos. 8 and 22) at the middle position of the fourth blade of the toroidal ALT-II limiter, two (the top and the bottom) from five bumper limiters and two from the main poloidal limiter (one from the top and one from the bottom) which are vacuum plasma sprayed (VPS) – W (0.5 mm thickness) coated graphite blocks. The locations and configurations of the limiter tiles are shown in Fig. 1. Both the ALT-II limiter and bumper limiter were used in the term from the middle of 1998 to the middle of 1999 and exposed to more than ten thousands shots, whereas the poloidal limiter was only used for high-Z experimental campaign with several tens of shots.

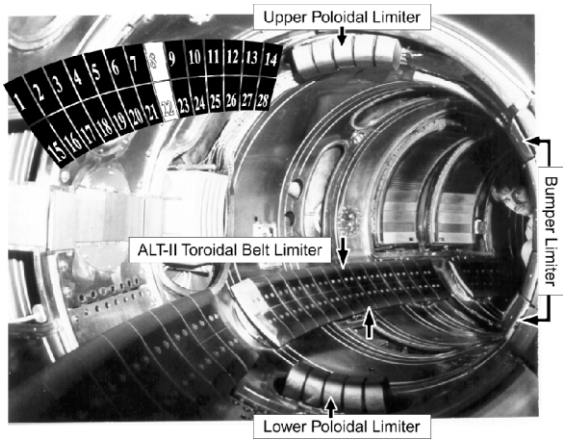

Fig. 1. Photograph of TEXTOR-94 vacuum vessel with ALT-II toroidal belt limiters, bumper limiters and VPS-W coated poloidal limiters. Two tiles of nos. 8 and 22 at blade 4 of ALT-II limiters, two (the top and the bottom) of the bumper limiters and two poloidal limiters situated at upper and lower part of vessel were investigated.

The imaging plate (hereafter referred as to IP) used here was BAS-TR2025 for low energy β-rays emitter such as tritium, manufactured by Fuji Photo Film. The surface of IP was exposed to the graphite tiles with a face-to-face contact for a week in a dark shielded room. After the exposure, IP was processed by an imaging plate reader, Fuji BAS-2000 or BAS-2500 to obtain digitized intensity mapping called a radioluminograph. The pixel size of the radioluminograph was set to be 100×100 μm^2.

In order to confirm that the recorded radioluminograph is entirely due to tritium, IP was exposed to the sample with inserting a polyimide film of 7.5 μm thickness between IP and the sample, which inhibited the β-electron penetration from tritium to IP but allowed the transport of X- and γ-rays. Thus all radioluminographs presented here represent tritium areal distribution within 5 μm from the surface. (The average projected range of 18.6 keV tritium β-electron is estimated to be about 5 μm from the surface.)

3. Results

3.1. ALT-II toroidal limiter

Fig. 2 compares the photograph with the radioluminograph of one of the ALT-II limiter tile (no. 22). Vertical and horizontal directions in Fig. 2 correspond to the poloidal and toroidal direction, respectively. Two holes in the central area are for the fixing bolts to the base plate. One can see an excellent correspondence in shape between the photograph and the radioluminograph. The lower, larger part of the tile is an erosion-dominated region and the upper part with rough surface is a deposition-dominated region covered with redeposited layers of 10–20 μm [8]. Tritium distribution at the erosion-dominated region is rather homogeneous and much higher than that at the deposition-dominated region. However, by peeling off some area of the deposited layer, the tritium level beneath the deposited layer was found to be very similar or a little higher than that of the erosion-dominated region as shown in Fig. 2(c). Tritium was also detected even on the backside where there was some space against the back plate.

Fig. 2(d) and (e) are tritium line profiles parallel to the toroidal direction and poloidal direction, respectively. The line profile shows that the tritium level beneath the deposited layer is also very homogeneous and a little higher than on the erosion-dominated region. The results for another tile (no. 8) were quite similar except a little higher tritium concentration (not shown here).

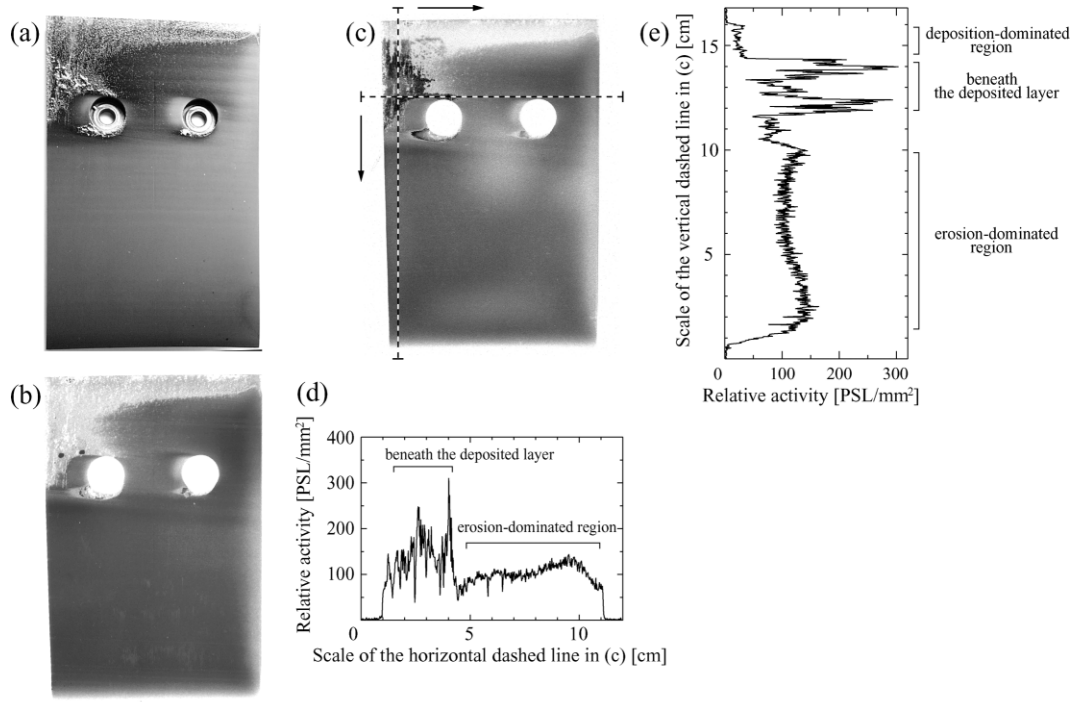

Fig. 2. (a) Photograph of a ALT-II toroidal limiter tile (blade 4, no. 22), (b) radioluminograph of the tile, (c) radioluminograph of the tile after peeling off some part of deposited layers, (d) tritium line profile on the horizontal dashed line drawn in (c) and (e) tritium line profile on the vertical dashed line drawn in (c). Tritium level becomes higher from white to black in the radioluminographs.

3.2. Bumper limiter

Fig. 3 shows photographs of the bottom and top bumper limiters and corresponding radioluminographs. Because of the curved shape to the toroidal direction, the tritium level of the electron drift side is a little higher than that of the ion drift side due to a shadowing effect. The figure also shows that the tritium density on the surface of the bottom tile is higher than the top one. Tritium was also detected even at the backside of the bumper limiters.

3.3. Poloidal limiter

Fig. 4(a) shows one of the bottom VPS-W coated poloidal limiters. Due to an extremely high and inhomogeneous heat load [9], the VPS-W coating partly melted indicating the surface temperature being over 3500 K. It was hardly possible to make a radioluminograph from the front surface, because of the curvature. But the tritium level of the melted region was found to be quite low, so dose the other high temperature region. It is of very interest to know that both sides of the limiter, which were not directly faced to the plasma, retained significant amount of tritium as shown in Fig. 4(b)–(d). They compare the side views of both the top and the bottom poloidal limiter to corresponding radioluminographs with a tritium line profile. The tritium level is quite consistent with a temperature profile during the shots, high for both edges (lower temperature regions), lower at the central (high temperature) region and lowest at the W-melted region. The results for the top VPS-W coated poloidal limiter were very similar to the bottom one, except less tritium amount retained.

Although the total exposure time of the poloidal limiter to the plasma was much less than that of the ALT-II limiter, the tritium level found in the former is only a little smaller than that in the latter.

4. Discussion

It is very interesting to note that the tritium distribution on the ALT-II tiles is quite homogeneous, compared to the deuterium distribution [8]. The reason is in the following.

The incident energy of deuterium from the boundary plasma to the limiters is several tens of electronvolt and the deuterium is thus implanted within only several nanometer from the surface. On the erosion-dominated region, such thin layer is readily eroded and the deuterium concentration at this region cannot be high. On the

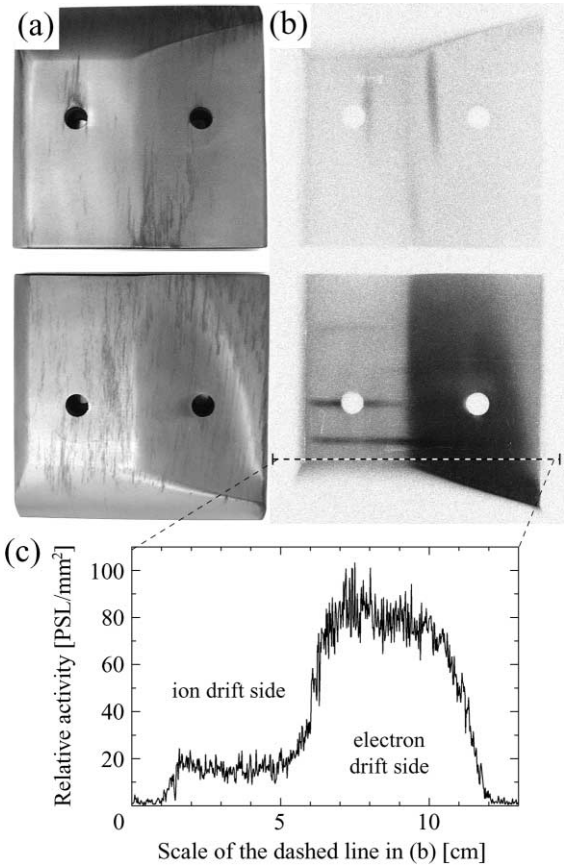

Fig. 3. (a) Photograph of the bumper limiter tiles and (b) corresponding radioluminographs with (c) tritium line profile on the dashed lines drawn in (b). The top and the bottom in the radioluminograph correspond the tiles at respective positions in the five bumper limiter tiles fixed at the TEXTOR vacuum vessel.

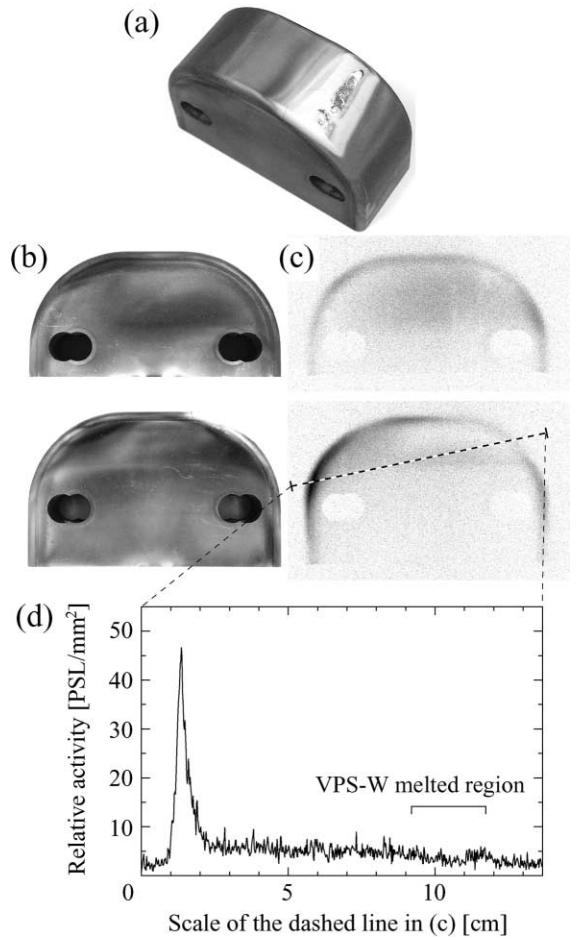

Fig. 4. (a) Photograph of one of VPS-W coated poloidal limiters situated at the bottom of the TEXTOR, (b) side views of VPS-W coated graphite tiles from the bottom and the top of the poloidal limiters, and (c) corresponding radioluminographs with tritium line profile given in (d). Melting of the tungsten layer is appreciable in (a).

other hand, the deuterium concentration in the deposited layer is very high (0.1–0.2 in D/C ratio [10]), due to the continuous deposition of deuterium with carbon during plasma discharges.

Different from deuterium, tritium generated by the D–D reaction in plasma has a maximum energy of 1.01 MeV

$$\mathrm{D} + \mathrm{D} \rightarrow \mathrm{T}(1.01\ \mathrm{MeV}) + p(3.03\ \mathrm{MeV}) \cdots 50\%$$
$$\mathrm{D} + \mathrm{D} \rightarrow {}^{3}\mathrm{He}(0.82\ \mathrm{MeV}) + n(2.45\ \mathrm{MeV}) \cdots 50\%$$

Considering the plasma volume of TEXTOR (2.7 and 0.46 m in major and minor radius) and the toroidal field strength of 2.2 T, the 1.01 MeV tritium atoms are not likely to lose fully their energies in the plasma and impinge into the limiters with rather high energies. In addition, the high-energy tritium gyrates along the magnetic field lines with a large gyro radius of 11 cm at maximum. Thus the tritium impinges uniformly everywhere on the limiter tiles even on the backside, if there is sufficient space between the tiles and the back plate. This is the reason for the very homogeneous tritium distribution.

The difference in the tritium level between the erosion-dominated region and the deposition-dominated region can be explained as follows. Although the maximum implantation depth of the 1.01 MeV tritium in graphite is about 10 μm, the tritium distributes shallower region due to the small incidence angles of magnetic field lines and its gyration. Therefore, most of the tritium would be within the depth detection limit of the tritium by means of TIPT, about 5 μm. The thickness of the deposited layer was reported to be 12 μm in average [8]. Although the eroded thickness is not clear, it is likely

much smaller than the thickness of the deposited layer. On the deposition-dominated region, the deposition and implantation proceed simultaneously. Owing to the large implanted depth of tritium, however, the deposited layer does not work as a barrier but its growth makes the implanted profile more flat. On the erosion-dominated region, the erosion and implantation proceed simultaneously. Again the larger implanted depth, compared to the erosion depth, makes most of the tritium remain with the depth profile a little flattened. Hence the tritium level on the erosion-dominated region becomes high compared to that on the deposition-dominated region.

According to Matsuyama et al. [11], the absolute amount of implanted tritium in ALT-II tiles is about 100 Bq/cm^2. The integrated neutron flux in the period from 1998 to 1999 was 3×10^{16} neutrons. According to the D–D reactions given above, the same amount of T as that of neutron should be produced resulting 53 MBq in total. Supposing this amount of tritium is homogeneously distributed to the whole surface area of a torus with 46 cm in diameter (The position of the ALT-II limiter is 46 cm from the plasmas center), the areal density of tritium is calculated to be about 109 Bq/cm^2, which agree quite well with the observed value.

The reason for a little higher density of tritium beneath the deposited layer than on the erosion-dominated region is in the following. During storage of the tiles in air before the measurements, tritium near surface could be removed by an isotope exchange reaction with hydrogen atoms in water, whereas the tritium beneath the deposited layer was protected by the layer.

Although the tritium distribution on two bumper limiters is rather homogeneous on each, tritium levels between them are clearly different. The difference of the tritium level was also seen between the bottom and the top of the poloidal limiters. This probably reflects the asymmetrical plasma character of TEXTOR-94. A separate measurement of Si collector probes, which were set at the bottom and the top of TEXTOR vacuum vessel, also showed clear difference, much higher tritium for the bottom specimen than for the top one.

The difference in tritium level should reflect the heat, or particle load at the ALT-II limiters and the poloidal limiters. According to the estimation of global heat load pattern on the ALT-II limiters [9], the heat load to the tile no. 8 was a little lower than that to the tile no. 22. While the tritium level of the former is a little higher than the latter. There is also a local temperature distribution in each tile, i.e., the temperature at leading edge of the all tiles (corresponding the bottom side in Fig. 2) is clearly higher than the temperature of the central area fixed at the base plate. The tritium distribution in Fig. 2(b) does not, however, show significant reduction of tritium level near the leading edge. Thus the cause of the small tritium distribution difference in ALT-II limiters is not clear at the moment.

On the other hand, at the poloidal limiter, where the surface temperature was significantly high, the tritium distribution is quite consistent with the temperature distribution. As a result, tritium remained only at lower temperature regions or both sides of the limiter, which were not directly exposed to the plasma (of course they were exposed to the gyrated ions). In addition, the exposure time to the plasma of the poloidal limiter was much less than that of the ALT-II limiter. Nevertheless, the tritium intensity of the former is very close or a little less than that of the latter. This may indicate that tritium is produced by target D–D reaction under high flux and rather high incident energy of deuterium to the poloidal limiter.

5. Conclusions

TIPT is demonstrated to be very effective for tritium mapping. Applying TIPT to tritium mapping of graphite tiles used in TEXTOR limiters, we have successfully obtained a lot of new information not only for tritium mapping but also for plasma-material interactions as follows.

1. Tritium distribution on the ALT-II tiles was found to be quite homogeneous. This is because high-energy tritium cannot lose its energy fully and implanted into the tiles with rather large gyration. By comparing different tiles, there is a certain difference in their tritium levels corresponding to heat load pattern on the ALT-II limiters, i.e., lower tritium for higher heat load.
2. Tritium in the deposited layer is much less than that in the erosion dominated area, quite opposite to the deuterium distribution.
3. Tritium level is higher at the bottom half of the torus than at the top half, reflects the asymmetrical plasma character of TEXTOR-94.
4. At extremely high particle loaded area, tritium is likely produced by target D–D reaction.

Acknowledgements

The authors wish to thank emeritus Professor C. Mori and Dr A. Uritani, Nagoya University for their kind suggestion and assistance for tritium imaging.

References

[1] G. Federici, R.A. Anderl, P. Andrew, J.N. Brooks, R.A. Causey, J.P. Coad, D. Cowgill, R.P. Doerner, A.A. Haasz, G. Janeschitz, W. Jacob, G.R. Longhurst, R. Nygren, A. Peacock, M.A. Pick, V. Philipps, J. Roth, C.H. Skinner, W.R. Wampler, J. Nucl. Mater. 266–269 (1999) 14.

[2] P. Andrew, P.D. Brennan, J.P. Coad, J. Ehrenberg, M. Gadeberg, A. Gibson, D.L. Hillis, J. How, O.N. Jarvis, H. Jensen, R. Lässer, F. Marcus, R. Monk, P. Morgan, J. Orchard, A. Peacock, R. Pearce, M. Pick, A. Rossi, P. Schild, B. Schunke, D. Stork, Fus. Eng. Des. 47 (1999) 233.
[3] C.H. Skinner, W. Blanchard, J.N. Brooks, J. Hogan, J. Hosea, D. Mueller A. Nagy, in: Proceedings of the 20th Symposium on Fusion Technology, Marseille, vol. 1, 7–11 September 1998, p. 153.
[4] G.R. Caskey, in: N.F. Fiore, B.J. Berkowitz (Eds.), Advanced Techniques for Characterizing Hydrogen in Metals, The Metallurgical Society of AWE, 1982, p. 61.
[5] M. Sonoda et al., Radiology 148 (1983) 833.
[6] Y. Amemiya, J. Miyahara, Nature (Lond.) 336 (1988) 89.
[7] C. Mori, private communication.
[8] P. Wienhold, H.G. Esser, D. Hildebrandt, A. Kirschner, K. Ohya, V. Philipps, M. Rubel, J. von Seggern, Phys. Scr. T 81 (1999) 19.
[9] T. Denner, K.H. Finken, G. Mank, N. Noda, Nucl. Fus. 39 (1999) 83.
[10] M. Rubel, J. von Seggern, P. Karduck, V. Philipps, A. Vevecka-Priftaj, J. Nucl. Mater. 266–269 (1999) 1185.
[11] M. Matsuyama, T. Tanabe, N. Noda, V. Philipps, K.H. Finken, K. Watanabe, these Proceedings.